



HAL
open science

Phononic bandgap guidance of acoustic modes in photonic crystal fibers

Vincent Laude, Abdelkrim Khelif, Sarah Benchabane, Mikael Wilm, Thibaut Sylvestre, Bertrand Kibler, Arnaud Mussot, John M. Dudley, Hervé Maillotte

► **To cite this version:**

Vincent Laude, Abdelkrim Khelif, Sarah Benchabane, Mikael Wilm, Thibaut Sylvestre, et al.. Phononic bandgap guidance of acoustic modes in photonic crystal fibers. *Physical Review B: Condensed Matter and Materials Physics* (1998-2015), 2005, 71, pp.045107. hal-00001404

HAL Id: hal-00001404

<https://hal.science/hal-00001404>

Submitted on 3 Apr 2004

HAL is a multi-disciplinary open access archive for the deposit and dissemination of scientific research documents, whether they are published or not. The documents may come from teaching and research institutions in France or abroad, or from public or private research centers.

L'archive ouverte pluridisciplinaire **HAL**, est destinée au dépôt et à la diffusion de documents scientifiques de niveau recherche, publiés ou non, émanant des établissements d'enseignement et de recherche français ou étrangers, des laboratoires publics ou privés.

Phononic bandgap guidance of acoustic modes in photonic crystal fibers

Vincent Laude, Abdelkrim Khelif, Sarah BENCHABANE, and Mikael Wilm
*Département LPMO, Institut FEMTO-ST, CNRS UMR 6174, Université de Franche-Comté,
32 avenue de l'Observatoire, F-25044 Besançon cedex, France*

Thibaut Sylvestre, Bertrand Kibler, Arnaud Mussot, John M. Dudley, and Hervé Maillotte
*Département d'Optique P. M. Duffieux, Institut FEMTO-ST, CNRS UMR 6174,
Université de Franche-Comté, 16 route de Gray, F-25030 Besançon cedex, France*

The existence of guided elastic modes in a photonic crystal fiber for an arbitrary cross-section is demonstrated using waveguide finite element analysis. In particular, it is shown that band-gaps exist for guided elastic modes along the longitudinal fiber axis, and thus a photonic crystal fiber can be simultaneously a phononic crystal fiber. The introduction of a defect within the two-dimensional crystal leads to the formation of highly localized elastic waveguide modes that co-propagate in the same core volume as the guided optical mode. We consider the application of these properties to the suppression of stimulated Brillouin scattering, and to enhanced collinear acousto-optical interactions.

PACS numbers: 42.70.Qs, 63.20.-e, 42.65.Es, 78.20.Hp

The study of wave propagation in micro- and nano-structured materials is a subject of intense current research in physics. Much attention has focussed on electromagnetic wave propagation in photonic crystals and photonic crystal optical fibers (PCF) [1–3], but important results on acoustic wave interactions in phononic crystals have also been obtained [4, 5]. From a fundamental viewpoint, both phononic and photonic crystals possess remarkable guidance properties such as the existence of absolute band-gaps that forbid the propagation of waves in any direction, which has already led to a number of important applications in both the photonics and acoustics fields.

Most previous studies, however, have considered the phononic and photonic properties of periodically structured materials independently, although recent works have considered the novel possibility of enhanced photon-phonon interactions within acoustic one-dimensional band-gap materials [6, 7]. For the particular case of PCFs, phononic bandgaps have also been recently studied in a preform, but only for localized in-plane elastic waves across the transverse fiber cross-section [8]. The analysis of these modes was performed using both Rayleigh [8] and finite-difference time-domain [9] methods, but only for the two-dimensional in-plane bandgap case. No studies to date have considered the existence of phononic bandgaps for out-of-plane elastic guided modes along the longitudinal fiber axis. The existence of acoustic band-gaps for out-of-plane propagation in a two-dimensional solid-solid phononic crystal has, however, been recently demonstrated using a plane-wave expansion approach [10]. In this Letter, we study a novel combination of the acoustical and optical waveguiding properties in PCFs. By considering the full three-dimensional case of both in-plane and out-of-plane elastic wave propagation, an analysis of phononic-bandgap modes in a PCF is performed. This yields new insights into the physics and properties of micro-nano structures supporting phononic-bandgap guidance of elastic modes whilst simultaneously presenting single-mode optical

guidance in the same PCF core region. We then discuss particular design examples that lead to the hypersonic band-gap inhibition of stimulated Brillouin scattering, and the hybrid guidance of both acoustic and optical waves for enhanced acousto-optic interactions.

PCF is typically based on a periodic arrangement of micron-size cylindrical parallel air holes inside a silica matrix, with a central defect acting as a core. Light is guided along the solid or hollow core either by a photonic band gap effect [11] or by modified total internal reflection [12], respectively. As regards the propagation of elastic waves, the elastic energy vanishes within the hollow cylinders and is thus constrained to remain within the silica. The boundaries of the hollow cylinders can be considered as free from tractions and act as very efficient scatterers for elastic waves of any polarization. Our analysis of the elastic modes is based on the waveguide finite element method (FEM) which combines a plane-wave-like ansatz for modes along the assumed infinite propagation direction with a finite element approach that is advantageous in allowing the modelling of arbitrary cross-sections [13]. With this technique, the two-dimensional waveguide section in the plane (x, y) is meshed using finite elements, and the displacements are represented by piece-wise polynomials within the elements. Along the propagation direction z (aligned with the PCF axis) a sinusoidal variation of the displacements is imposed with a given wavevector k . To account for acoustic propagation along the z axis, a harmonic dependence $\exp(j(\omega t - kz))$ is considered. For isotropic materials and a cylindrical geometry, the coupling between the transverse components u_x and u_y and the longitudinal component u_z of the displacements includes a $\pm\pi/2$ dephasing. In order to guarantee a unique solution to the variational problem, we use the real-valued formulation within each finite element

$$u_x(x, y, z; t) = \mathbf{p}(x, y)^T \cdot \hat{\mathbf{u}}_x \cos(\omega t - kz), \quad (1)$$

$$u_y(x, y, z; t) = \mathbf{p}(x, y)^T \cdot \hat{\mathbf{u}}_y \cos(\omega t - kz), \quad (2)$$

$$u_z(x, y, z; t) = \mathbf{p}(x, y)^T \cdot \hat{\mathbf{u}}_z \sin(\omega t - kz), \quad (3)$$

where $\hat{\mathbf{u}} = (\hat{\mathbf{u}}_x, \hat{\mathbf{u}}_y, \hat{\mathbf{u}}_z)^T$ is the vector of the $3n$ displacements at the n nodes of the finite element and the \mathbf{p} is a vector of n Lagrange interpolation polynomials. The dynamics of elastic waves are obtained as the solution of a variational problem involving the kinetic and strain energies. The kinetic energy in a one-wavelength-long finite element with section \mathcal{S} is

$$\mathcal{K} = \omega^2 \int_0^{2\pi/k} dz \int_{\mathcal{S}} dx dy \mathbf{u}^T \cdot \rho \cdot \mathbf{u}, \quad (4)$$

where ρ is the mass density. Inserting Eqs. (1-3) and integrating along z yields $\mathcal{K} = \omega^2/2k (\hat{\mathbf{u}}^T \cdot M_S \cdot \hat{\mathbf{u}})$, with the elementary mass matrix M_S and the polynomial matrix P defined by

$$M_S = \int_{\mathcal{S}} dx dy P^T \cdot \rho \cdot P, \quad P = \begin{pmatrix} \mathbf{p}^T & 0 & 0 \\ 0 & \mathbf{p}^T & 0 \\ 0 & 0 & \mathbf{p}^T \end{pmatrix}. \quad (5)$$

Similarly, the strain energy within the finite element is given by

$$\mathcal{U} = \int_0^{2\pi/k} dz \int_{\mathcal{S}} dx dy S_I C_{IJ} S_J, \quad (6)$$

where the strain tensors S and C are written in contracted notation, i.e. C is a 6×6 matrix and S is a 6-component vector. Integrating along z and making use of sine and cosine orthogonality, the strain energy can be expressed as $\mathcal{U} = 1/2k (\hat{\mathbf{u}}^T \cdot K_S \cdot \hat{\mathbf{u}})$, with the elementary stiffness matrix defined as

$$K_S = \int_{\mathcal{S}} dx dy (A_r^T \cdot C \cdot A_r + A_i^T \cdot C \cdot A_i), \quad (7)$$

where

$$A_r = \begin{pmatrix} \mathbf{p}_{,x}^T & 0 & 0 \\ 0 & \mathbf{p}_{,y}^T & 0 \\ 0 & 0 & k\mathbf{p}^T \\ \mathbf{p}_{,y}^T & \mathbf{p}_{,x}^T & 0 \\ 0 & 0 & 0 \\ 0 & 0 & 0 \end{pmatrix}, \quad A_i = \begin{pmatrix} 0 & 0 & 0 \\ 0 & 0 & 0 \\ 0 & 0 & 0 \\ 0 & 0 & 0 \\ 0 & -k\mathbf{p}^T & \mathbf{p}_{,y}^T \\ -k\mathbf{p}^T & 0 & \mathbf{p}_{,x}^T \end{pmatrix}, \quad (8)$$

and the vectors $\mathbf{p}_{,x}^T = (\partial p_1/\partial x, \dots, \partial p_n/\partial x)$ and $\mathbf{p}_{,y}^T = (\partial p_1/\partial y, \dots, \partial p_n/\partial y)$. As is usual with elastic FEM problems, the solution of the variational problem with no external applied forces is given by the linear equation

$$(K(k) - \omega^2 M) \hat{\mathbf{u}} = 0 \quad (9)$$

where the stiffness matrix $K(k)$ and the mass matrix M are obtained by assembling the elementary stiffness and mass matrices respectively by standard procedures [14]. $K(k)$ is actually a second order matrix polynomial in k , while M is k -independent. Eq. (9) is in the form of a generalized eigenvalue problem for ω^2 if k is considered a parameter.

We have used this waveguide FEM technique to analyse the phononic bandgap characteristics of the silica-air honeycomb structures shown in meshed cross-section as insets in Fig. 1. Note that here, as elsewhere in this paper, open circles are associated with air holes. We show honeycomb structures both (a) without and (b) with a central solid silica defect. For this structure having a hole pitch (centre-to-centre distance) of a , the PCF diameter is then $\approx 10a$. The band structure in Fig. 1a for elastic waveguide modes without a central defect exhibits high density except in several regions where only isolated branches exist. An examination of the corresponding eigenvectors reveals that in the dense regions the elastic modes are similar to those of a solid cylinder. In particular, their energy density is spread in the whole fiber. In contrast, isolated branches correspond to modes that are localized on the external boundary of the PCF, which is clamped in the calculation. When the external boundary is considered stress-free instead, modes in the dense regions are only very slightly affected, but isolated branches are displaced. We interpret the isolated branches as corresponding to modes that are trapped between the external boundary of the PCF and the band gaps

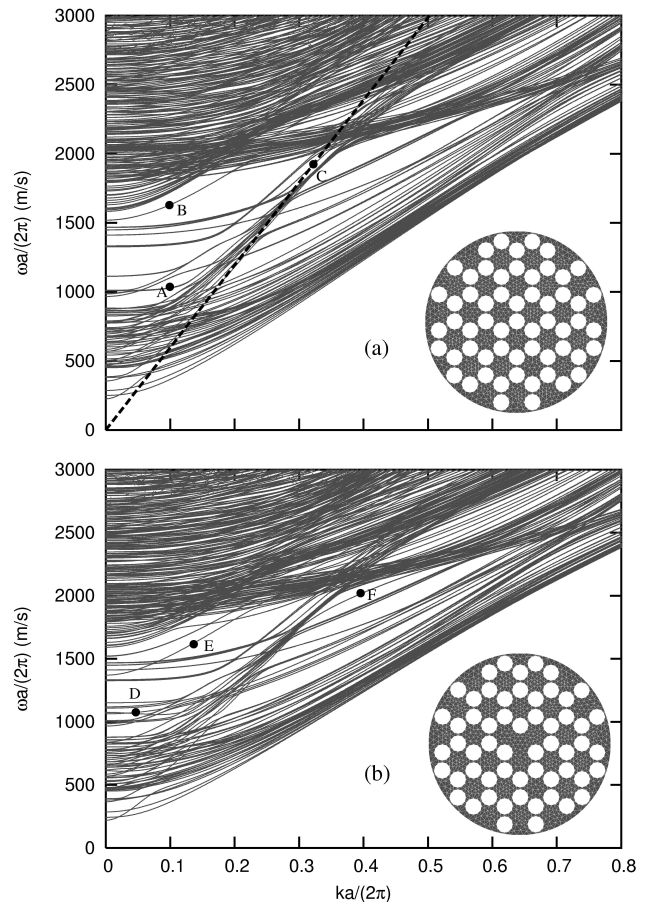


FIG. 1: Band structures for elastic waveguide modes of honeycomb silica PCFs (a) without and (b) with a central defect. The two-dimensional meshes of the cross-sections are shown as insets. The longitudinal line in silica is shown in (a).

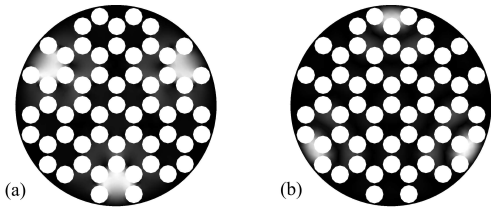


FIG. 2: Elastic guided modes (shown in grayscale) propagating along the external boundary of the PCF of Fig. 1a. (a) In-plane and (b) longitudinal displacements for the points labeled respectively (A) and (B) in Fig. 1.

of the inner honeycomb structure, as illustrated by Fig. 2.

Significantly, we have found that such honeycomb structures associated with out-of-plane phononic bandgaps can be combined with optically guiding PCF microstructures to raise the exciting possibility of hybrid phononic-photon guidance within a common mode area. As a first possible application, we consider a typical high-air-fraction PCF, usually used for optical guidance via modified total internal reflection, whose solid core is nanostructured by the defect-free honeycomb pattern in Fig. 1a, such that the nanostructured core presents a phononic bandgap engineered to inhibit stimulated Brillouin scattering (SBS). This is of much practical significance around the technologically-important wavelength range around 1550 nm as SBS is highly detrimental for fiber communications systems [15].

SBS is a three-wave nonlinear interaction in which an intense, incident optical pump wave of frequency ω_p is backscattered into a downshifted Stokes wave of frequency $\omega_s = \omega_p - \omega$ through the coherent generation of an acoustic phonon at frequency ω via material electrostriction [16]. The scattered acoustic phonons modulate the refractive index of the medium, acting as a Bragg grating propagating forward at the longitudinal acoustic velocity v , so that the reflected optical mode is downshifted through the Doppler effect. The longitudinal wave vector of the SBS phonon is given by the phase matching condition, $k = k_p - k_s$, where k_p and k_s are the optical pump and Stokes wavevectors, and $\omega = vk$ defines the SBS phonon dispersion relation. In silica, $v = 5970$ m/s which is much smaller than the speed of light, so that the acoustic wave vector and the SBS hypersound frequency are very well approximated in single-mode fibers by $k = 2k_p$ and $\omega = 2nv\omega_p/c$, where n is the effective index of the optical mode [15]. Using typical parameters for telecommunication fibers at $1.55 \mu\text{m}$, the acoustic wavelength and frequency are respectively 543 nm and 11 GHz. In general, optically-guiding high air-fraction PCFs will be acoustically multi-mode for such small acoustic wavelengths, but if a central additional nanostructure is added in the PCF core region to open an out-of-plane phononic bandgap for the phonon couple (ω, k) , the coherent amplification of SBS phonons will be inhibited.

To illustrate this more explicitly, the straight line in Fig. 1a passing through the origin shows the SBS phonon dispersion

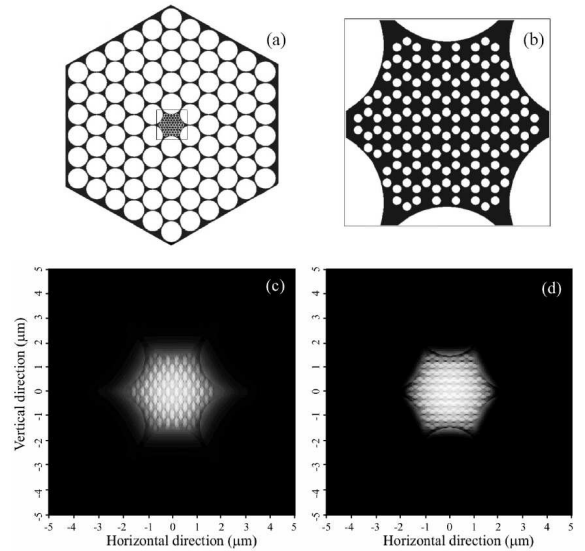


FIG. 3: (a) PCF cross-section showing the combined micro-nanostructure designed for simultaneous core optical guidance and the inhibition of SBS phonon propagation. (b) Detail of the core region. (c) and (d): Numerical simulations of the fundamental TE and TM optical modes at $1.55 \mu\text{m}$.

relation. Point (C) in Fig. 1a corresponds to $\omega a/(2\pi) = 1911$ m/s and $ka/(2\pi) = 0.32$, and illustrates that it is indeed possible to open phononic bandgaps around particular SBS phonon couples. Although it appears from the figure that the nanostructure opens up only a partial out-of-plane bandgap, the bandgap width can in fact be significantly larger than the SBS linewidth so that it is indeed possible to incorporate a suitably scaled honeycomb nanostructure within an exterior PCF microstructure such that highly confined optical guidance and SBS inhibition can be simultaneously obtained. In particular, we consider the mixed micro-nano PCF structure in Fig. 3a and Fig. 3b. Here, the hole diameter and pitch are $2.59 \mu\text{m}$ and $2.76 \mu\text{m}$ respectively for the exterior microstructure (typical solid core PCF dimensions) and 145 nm and 207 nm respectively for the internal honeycomb (technologically feasible sizes [3]). Simultaneous optical guidance in such a structure was verified using standard beam propagation method vector simulations, and Fig. 3c and Fig. 3d show the guided mode solutions for the TE (horizontal) and TM (vertical) electric field components. This illustrates that efficient optical guidance at $1.55 \mu\text{m}$ is indeed obtained in the presence of the phononic nanostructure. Calculation of the associated effective indices ($n = 1.2046$ and $n = 1.1557$ respectively) allows us to verify that the phononic bandgap is indeed opened about a mean SBS frequency of 9.3 GHz for both polarizations. Significantly, we can also see from Fig. 1a that the elastic band-gap width is much wider than the usual SBS linewidth of 50 MHz [15], thus ensuring complete SBS phonon inhibition. We note that, contrary to current modulation techniques used to suppress SBS in optical fibers that often impair the overall transmission performance, the proposed

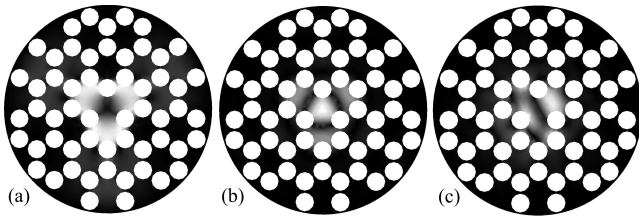


FIG. 4: Elastic waveguide modes (shown in gray-scale) localized in the core of the PCF of Fig. 1b by a phononic band-gap effect. (a) In-plane and (b-c) longitudinal displacements for the points labeled respectively (D), (E), and (F) in Fig. 1b.

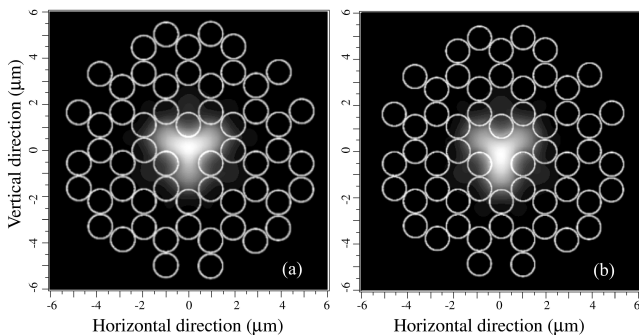


FIG. 5: Optical (a) TE and (b) TM modes simulations in the same PCF as in Fig. 4.

nanostructuring of a PCF is totally passive.

Our waveguide FEM technique also allows the convenient investigation of a range of other photo-phononic structures, and we consider now the phononic bandgap properties of the structure previously shown in Fig. 1b, of which the central silica defect is expected to introduce localized elastic modes within the band-gaps. A comparison of the band structures of Figs. 1a and 1b reveals that the densely populated mode regions, as well as the isolated branches corresponding to modes localized between the external boundary and the honeycomb-structured interior are very similar, indicating insensitivity of these modes to the presence of the core defect. However, it is significant that additional isolated branches appear within the band-gaps in Fig. 1b, and examination of modes along these particular branches reveals that they are localized and trapped within the silica defect, as illustrated by Fig. 4. Waveguiding of these elastic core modes clearly relies on the out-of-plane elastic band-gap properties of the PCF. Beam propagation method simulations were again used to check that optical core guidance is possible under realistic conditions. Fig. 5a and Fig. 5b show the fundamental optical TE and TM modes at $1.55 \mu\text{m}$, respectively for a hole diameter and pitch of $1.01 \mu\text{m}$ and $1.13 \mu\text{m}$. With such dimensions, the frequency of the acoustic waveguide mode of Fig. 4b (corresponding to point (E) in Fig. 1b) is 1.3 GHz. Hence, from Fig. 4 and Fig. 5,

we anticipate that guided acoustic modes within such an out-of-plane phononic band-gap structure will enable enhanced collinear acousto-optical interactions, presenting both a significantly increased interaction length compared to in-plane acousto-optical interactions across the PCF cross-section [8] and the possibility of coherently coupling and transferring energy between several optical modes. By controlling the anisotropy of the PCF, e.g. through the anisotropic distribution of holes, anisotropic acousto-optical interaction between optical modes of different polarization should also be possible. Such an interaction may for instance find applications in ultrashort laser pulse shaping, as an alternative to bulk acousto-optical programmable filters [17].

In summary, we have demonstrated that out-of-plane phononic band-gaps exist in a PCF with an arbitrary finite cross-section, raising the possibility of guiding elastic modes localized along the external boundary of the PCF as well as inside a defect of the phononic crystal. Based on these features, hybrid guidance of acoustic and optical guided modes has been demonstrated within a PCF simultaneously forming a phononic crystal fiber. This property yields new insights into the possibility of enhanced acousto-optical interactions, as well as inhibition of light-induced acoustic waves like stimulated Brillouin scattering.

-
- [1] E. Yablonovitch, Phys. Rev. Lett. **58**, 2059 (1987).
 - [2] S. John, Phys. Rev. Lett. **58**, 2486 (1987).
 - [3] P. S. J. Russell, Science **299**, 358 (2003).
 - [4] M. M. Sigalas and E. N. Economou, Solid State Commun. **86**, 141 (1993).
 - [5] M. S. Kushwaha, P. Halevi, L. Dobrzynski, and B. Djafari-Rouhani, Phys. Rev. Lett. **71**, 2022 (1993).
 - [6] J. M. Worlock and M. L. Roukes, Nature **421**, 802 (2003).
 - [7] M. M. de Lima, Jr., R. Hey, and P. V. Santos, Appl. Phys. Lett. **83**, 2997 (2003).
 - [8] P. S. J. Russell, E. Marin, A. Diez, S. Guenneau, and A. B. Movchan, Opt. Express **20**, 2555 (2003).
 - [9] A. Khelif, B. Djafari-Rouhani, V. Laude, and M. Solal, J. Appl. Phys. **94**, 7944 (2004).
 - [10] M. Wilm, A. Khelif, S. Ballandras, V. Laude, and B. Djafari-Rouhani, Phys. Rev. E **67**, 065602(R) (2003).
 - [11] R. F. Cregan, B. J. Mangan, J. C. Knight, T. A. Birks, P. S. J. Russell, P. J. Roberts, and D. C. Allan, Science **285**, 1537 (1999).
 - [12] T. A. Birks, J. C. Knight, and P. S. Russell, Opt. Lett. **22**, 961 (1997).
 - [13] B. Aalami, J. of Appl. Mech. **40**, 1067 (1973).
 - [14] O. C. Zienkiewicz and R. L. Taylor, *Finite Element Method* (Butterworth Heinemann, London, 2000).
 - [15] G. P. Agrawal, *Nonlinear Fibers Optics, 3rd Ed.* (Academic, San Diego, 2001).
 - [16] R. Y. Chiao, C. H. Townes, and B. P. Stoicheff, Phys. Rev. Lett. **12**, 592 (1964).
 - [17] F. Verluise, V. Laude, Z. Cheng, C. Spielmann, and P. Tournois, Opt. Lett. **25**, 575 (2000).